Electrochemical Bioassay Utilizing Encapsulated Electrochemical Active Microcrystal Biolabels

ARTICLE *in* ANALYTICAL CHEMISTRY · JUNE 2005

Impact Factor: 5.64 · DOI: 10.1021/ac048505l · Source: PubMed

6 AUTHORS, INCLUDING:

Wing Cheung Mak
Linköping University
41 PUBLICATIONS **707** CITATIONS
SEE PROFILE

Dieter Trau
National University of Singapore (NUS)
64 PUBLICATIONS **1,759** CITATIONS
SEE PROFILE

Reinhard Renneberg
The Hong Kong University of Science and Tec…
250 PUBLICATIONS **4,111** CITATIONS
SEE PROFILE

Anal. Chem. **2005,** *77,* 2835−2841

Electrochemical Bioassay Utilizing Encapsulated Electrochemical Active Microcrystal Biolabels

Wing Cheung Mak,*,†,‡ Kwan Yee Cheung,† Dieter Trau,§ Axel Warsinke,|| Frieder Scheller,|| and Reinhard Renneberg†

Sino-German Nano-Analytical Laboratory (SiGNAL), Department of Chemistry, and the Bioengineering Graduate Program, The Hong Kong University of Science and Technology, Clear Water Bay, Kowloon, Hong Kong, Department of Bioengineering and Department of Chemical and Biomolecular Engineering, National University of Singapore, Singapore, and Institute of Biochemistry and Biology, University of Potsdam, Karl-Liebknecht-Strasse 24−25, 14476 Golm, Germany

A new approach to perform electrochemical immunoassay based on the utilization of encapsulated microcrystal was developed. The microcrystal labels create a "supernova effect" upon exposure to a desired releasing agent. The microcrystal cores dissolve, and large amounts of signal-generating molecules diffuse across the capsule wall into the outer environment. Layer-by-Layer (LbL) technology was employed for the encapsulation of electrochemical signal-generating microcrystals (ferrocene microcrystals). The encapsulated microcrystals were conjugated with antibody molecules through the adsorption process. The biofunctionalized microcrystals were utilized as a probe for immunoassays. The microcrystal-based label system provided a high-signal molecule to antibody (*S*/*P*) ratio of 10^4-10^5. Microcrystal biolabels with different antibody surface coverage ($1.60-5.05$ mg m^{-2}) were subjected to a solid-phase immunoassay for the detection of mouse immunoglobulin G (M-IgG) molecules. The microcrystal-based immunoassay for the detection of M-IgG performed with microcrystals having antibody surface coverage of 5.05 mg m^{-2} showed a sensitivity of 3.93 nA μg^{-1} L^{-1} with a detection limit of 2.82 μg L^{-1}.

Immunoassays have been widely used as the standard technology for quantitative detection of analyte concentrations in the fields of medicine, environmental science, and food science. Photometric or colorimetric immunoassays based on enzyme-labeled antibodies are the most commonly used laboratory technique, which requires a photometer to read out the test result. Electrochemical immunoassay provides a possible tool for on-site or portable measurement by use of a microelectronic device such as an electrochemical transducer. Conventional electrochemical bioassay based on a ferrocene or heme-modified label system has the disadvantage of only a small number of redox-active labels (typically 3−10) are conjugated to one antibody or antigen molecule. An amplified label system based on a redox-active compound and enzyme-labeled antibody showed an improved assay performance. However, the enzyme-labeling system required the addition of external substrate and incubation procedure.

Various techniques for direct or indirect electrochemical immunoassays have been developed. Potentiometric, capacitive, and amperometric transducers have been employed for direct immunoassay for the detection of anti-dioxin antibodies,[1] polychlorinated biphenyls (PCBs),[2] anti-mouse immunoglobulin G,[3,4] and anti-human chorionic gonadotropin hormone (CGH) antibodies.[5] Although direct immunoassay provides the advantage of a label-free detection method, often sensitivity and the limit of detection cannot compete with label-based immunoassay methods. Antibodies or antigens are usually non-electrochemical-active. To generate a signal in an amperometric assay, the antibody (or antigen, depending on the assay format) is usually conjugated to a redox-active compound or enzyme. Redox-active compounds such as ferrocene or heme-modified antibodies have been applied for such indirect immunoassay. However, only a small number of redox-active labels are conjugated to one antibody or antigen molecule. They will generate a signal equivalent in current which is proportional to the number of redox molecules and transmitted electrons per redox reaction. As a result a current of only a few electrons is generated per antigen/antibody binding events, resulting in poor sensitivity and limit of detection. Conjugation of ferrocene molecules directly to antibodies has been used for the detection of histamine.[6] This method showed a good relationship for determination of the histamine concentration in the range from 200 to 2000 ng mL^{-1}. Antibodies conjugated with different enzymes such as glucose-6-phosphate dehydrogenase,[7] glucose oxidase,[8] catalase,[9] and peroxidase[10−12] has been applied for electrochemical immunoassay. However, the enzyme-conjugated

* Corresponding author. Telephone: +852−23587410. E-mail: chmartin@ust.hk.
† SiGNAL, Department of Chemistry, The Hong Kong University of Science and Technology.
‡ Bioengineering Graduate Program, The Hong Kong University of Science and Technology.
§ National University of Singapore.
|| University of Potsdam.

(1) Keating, M. Y.; Rechnitz, G. A. *Anal. Chem.* 1985, *56*, 801−806.
(2) Sadik, O. A.; VanEmon, J. M. *CHEMTECH* **1997**, *27*, 38−46.
(3) Gebbert, A.; Alvarez-Icaza, M.; Stoecklein, W.; Schmid, R. D. *Anal. Chem.* **1992**, *64*, 997−1003.
(4) Gebbert, A.; Alvarez-Icaza, M.; Peters, H.; Jager, V.; Bilitewski, U.; Schmid, R. D. *J. Biotechnol.* **1994**, *32*, 213−220.
(5) Berggren, C.; Johansson, G. *Anal. Chem.* **1997**, *69*, 3651−3657.
(6) Lim, T.; Tadashi, M. *Biosens. Bioelectron.* **2001**, *16* (9−12), 1063−1069.
(7) Athey, D.; McNeil, C. J.; Bailey, W. R.; Hager, H. J.; Mullen, W. H.; Russell, L. J. *Biosens. Bioelectron.* **1993**, *8*, 415−419.
(8) Robinson, G. A.; Cole, V. M.; Forrest, G. C. *Biosensors* **1988**, *3* (3), 147−160.
(9) Aizawa, M.; Morioka, A.; Suzuki, S. *Anal. Chim. Acta* **1980**, *115*, 61−67.
(10) Rishpon, J.; Ivnitski, D. *Biosens. Bioelectron.* **1997**, *12*, 195−204.

10.1021/ac048505l CCC: $30.25
Published on Web 03/26/2005

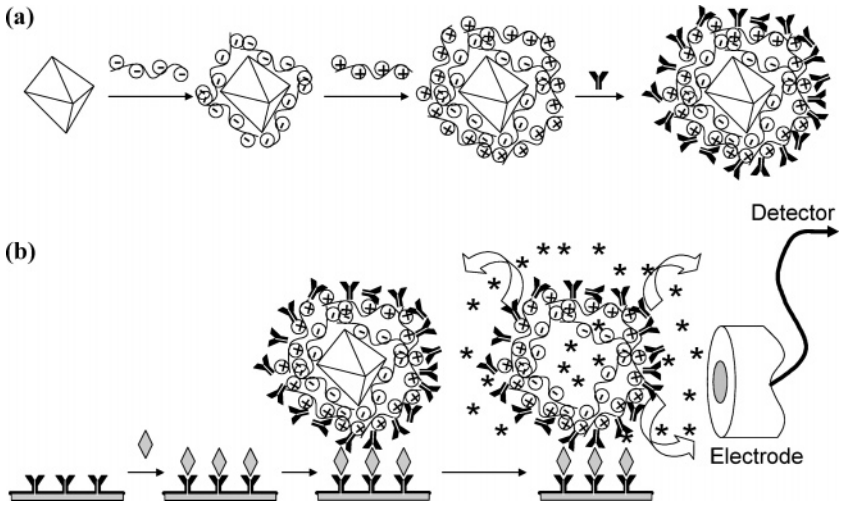

Figure 1. Schematic diagram illustrating (a) the preparation of microcrystal-labeled antibody conjugate And (b) the principle of microcrystal-labeled electrochemical immunoassay.

antibody system required the addition of external reagents and incubation procedures. More detailed examples for electrochemical immunoassay are discussed in a review paper by Warsinke et al.[13]

In this paper, a new approach for electrochemical immunoassays based on the utilization of encapsulated electrochemical signal-generating microcrystals (e.g., redox-active microcrystals) is described. The encapsulation of signal-generating molecules may give a push to new bioanalytical technologies. Liposome has been used for encapsulating various signal-generating molecules such as organic molecules (drugs and fluorophores), enzymes, enzyme substrates, DNA, and radioactive isotopes.[14] The resulted liposome labels can be conjugated with antibodies or antigens to perform homogeneous or heterogeneous immunoassay. In recent years, a new strategy on preparation and utilization of polymeric encapsulated microcrystalline fluorescein diacetate (fluorescence signal precursor) particles conjugated with antibodies as a probe for amplified biochemical assay has been described by Trau et al.[15] Moreover, encapsulations of different signal-generating molecules, e.g., fluorescent[16] and visible dyes,[17] enzymes,[18] antibodies,[19] and hormones[20,21] have been studied. The state-of-the-art layer-by-layer (LbL) technology provides a simple method to encapsulate a crystallized organic compound with tailored capsule properties. A high number of signal-generating molecules present in the microcrystal core were encapsulated with a polymeric capsule. The ultrathin and porous polymeric capsule wall provides an interface between the crystalline core and the outer aqueous environment. Such microcrystalline labels create a "supernova effect" upon exposure to a desirable releasing agent. The core crystal dissolves immediately, and huge amounts of signal-generating molecules diffuse across the capsule wall into the outer environment.

Ferrocene $Fe(C_5H_5)_2$ was employed as a model system for electrochemical signal-generating microcrystals. The encapsulation of ferrocene microcrystals was achieved by alternating the deposition of the polyelectrolyte multilayer via LbL technique. The polyelectrolyte-coated microcrystals were further coated with goat anti-mouse immunoglobulin G (Gt α M-IgG) antibodies as the outermost layer via adsorption. The resulted antibody-conjugated ferrocene microcrystals were used to perform a sandwich bioaffinity immunoassay for the detection of mouse immunoglobulin G (M-IgG), as shown in Figure 1. After binding of the microcrystal label detector, a releasing agent was added, resulting in the release of a large amount of electrochemical signal-generation molecules into the outer medium through the permeable capsule wall. The released electrochemical signal-generating molecules were then measured amperometrically.

EXPERIMENTAL SECTION

Materials. Poly(sodium 4-styrenesulfonate) (PSS, $\bar{M}_w \approx 70\,000$ g mol^{-1}), poly(allylamine hydrochloride) (PAH, $\bar{M}_w \approx 15\,000$ g mol^{-1}), bovine serum albumin (BSA), ferrocene, and dimethyl sulfoxide (DMSO) were purchased from Aldrich Chemical Co. Trizma base (Tris) and affinity-purified polyclonal mouse immunoglobulin G (M-IgG) and goat anti-mouse immunoglobulin G (Gt α M-IgG) were purchased from Sigma. Tween 20 was purchased from USB.

Assembly of Polyelectrolyte Multilayers onto Ferrocene Microcrystals. Ferrocene crystals (5 mg) were milled with 5 mg mL^{-1} PSS solution followed by sonication for 10 min. The

(11) Abdel-Hamid, I.; Ghindilis, A. L.; Atanasov, P.; Wilkins, E. *Anal. Lett.* **1999**, *32* (6), 1081−1094.
(12) Dai, Z.; Yan, F.; Chen, J.; Ju, H. *Anal. Chem.* **2003**, *75*, 5429−5434.
(13) Warsinke, A.; Benkert, A.; Scheller, F. W. *Fresenius' J. Anal. Chem.* **2000**, *366*, 622−634.
(14) Rongen, H. A. H.; Bennekom, A. W. P. *J. Immunol. Methods* **1997**, *204*, 105−133.
(15) Trau, D.; Yang, W.; Seydack, M.; Caruso, F.; Yu, N. T.; Renneberg, R. *Anal. Chem.* **2002**, *74*, 5480−5486.
(16) Caruso, F.; Yang, W.; Trau, D.; Renneberg, R. *Langmuir* **2000**, *16*, 8932−8936.
(17) Dai, Z.; Voigt, A.; Donath, E.; Möhwald, H. *Macromol. Rapid Commun.* **2001**, *22*, 756−762.
(18) Caruso, F.; Trau, D.; Möhwald, H.; Renneberg, R. *Langmuir* **2000**, *16*, 1485−1488.
(19) Shimizu, M.; Miwa, Y.; Hashimoto, K.; Goto, A. *Biosci., Biotechnol., Biochem.* **1993**, *32* (9), 1445−1449.
(20) Johnson, O. L.; Jaworowicz, W.; Cleland, J. L.; Bailey, L.; Charnis, M.; Duenas, E.; Wu, C.; Shepard, D.; Magil, S.; Last, T.; Jones, A. J.; Putney, S. D. *Pharm. Res.* **1997**, *14* (6), 730−735.
(21) Cleland, J. L.; Mac, A.; Boyd, B.; Yang, J.; Duenas, E. T.; Yeung, D.; Brooks, D.; Hsu, C.; Chu, H.; Mukku, V.; Jones, A. J. *Pharm. Res.* **1997**, *14* (4), 420−425.

suspension was allowed to stand for 30 min, thus allowing the large crystals to sediment. The suspended colloid microcrystals in the supernatant were extracted, centrifuged, washed two times with water, and finally resuspended in water. The first layer was adsorbed by addition of 2 mL of PAH solution (5 mg mL^{-1}, in 0.5 M NaCl), occasionally shaking and incubating for 20 min for adsorption. After the adsorption process, the suspension was centrifuged at 6200 rpm (3200*g*) for 2 min, and the excess polyelectrolyte was removed by two washing and redispersion cycles with water. Deposition of the next layer with PSS solution (5 mg mL^{-1}, in 0.5 M NaCl), bearing an opposite charge to that already adsorbed crystal surface was performed with similar procedures and conditions. The crystal surfaces were coated with polyelectrolyte multilayers by alternated deposition of PAH and PSS until the desired number of layers was achieved (typically eight layers). The encapsulated ferrocene microcrystals were kept at 4 °C in double distillated water for storage.

Preparation and Characterization of Microcrystal-Based Biolabels. Biofunctional ferrocene microcrystals were freshly prepared each time for experiment. Ferrocene microcrystals coated with $[PSS/PAH]_4$ were conjugated to Gt α M-IgG by adsorption. An aliquot of 400 μL encapsulated ferrocene suspension (~24.5 mg mL^{-1}) was added to 1 mL of Gt α M-IgG with various antibody concentrations ranged from 150 to 600 μg mL^{-1} in 0.05 M Tris-HCl at pH 7.4. The resultant mixture was incubated at 20 °C for 20 min with occasionally shaking. After the adsorption process, the antibody-conjugated ferrocene microcrystals were centrifuged at 6200 rpm (3200*g*) for 2 min, and the excess antibody was removed by two washing and redispersion cycles with Tris-HCl (pH 7.4). After the antibody conjugation process, the polymeric capsule surface was blocked by incubation with 1% (w/v) BSA in Tris-HCl (pH 7.4) for 5 min at 20 °C followed by two washing cycles with Tris-HCl.

The amount of antibody molecules adsorbed onto the microcrystal surfaces was determined by spectrophotometric measurement at 280 nm. After the antibody adsorption process, the antibody conjugated ferrocene microcrystals were precipitated by centrifugation. The antibody concentrations before adsorption and the antibody concentrations remain in the supernatant after the antibody adsorption process was subject to the spectrophotometric measurement. The different in the amount of antibody before and after adsorption process was calculated and represents the amount of antibody adsorbed onto the microcrystal surfaces.

Microcrystal-Labeled Sandwich Electrochemical Immunoassay. A Nunc Maxisorp 96-well microplate was coated with 100 μL per well Gt α M-IgG (1.2 μg mL^{-1}) in carbonate/bicarbonate buffer (pH 9.6).[22] The plate was incubated at 4 °C overnight. After incubation, the plate was washed four times with washing buffer (0.1 M phosphate buffer saline (PBS), 0.1% (w/v) BSA, 0.5% Tween-20). The plate was then blocked with 300 μL blocking buffer (0.5 M PBS, 1% (w/v) BSA) at 37 °C for 1 h. After blocking, the plate was washed four times with washing buffer. With concentrations ranging from 0 to 1.6 μg mL^{-1}, 100 μL analyte (M-IgG) solutions were added and washing buffer was used as the blank. The plate was incubated at 37 °C for 1 h followed by four times washing with washing buffer. An aliquot of 100 μL Gt α M-IgG conjugated ferrocene microcrystal suspension (~0.8 mg mL^{-1}) was added to each well and incubated at 37 °C for 1 h.[22] After incubation, the excess of ferrocene-labeled detector antibody was washed off four times with washing buffer. The dissolution of the particulate label (ferrocene microcrystals) resulted by addition of 50 μL of DMSO. The detection of the released electrochemical signal-generating molecules (ferrocene molecules) was measured amperometrically at +250 mV versus Ag/AgCl reference electrode.

Voltammetric and Amperometric Measurements. Cyclic voltammetric experiments were carried out using a BAS model 100B (W. Lafayette, IN) voltammetric analyzer interfaced with a personal computer and driven by BAS 100W version 2.0 software. A three-electrode configuration with a glassy-carbon working electrode, a platinum counter electrode and a silver/silver chloride (Ag/AgCl) reference electrode were used.

Amperometric experiments were carried out using an EP-30 (Biometra, Gottingen, Germany) electrochemical detector coupled with a computer system. Measurements were carried out at room temperature (20 °C) in phosphate buffer solution of pH 7.4 inside a stirring cell composed of a 10 mL plastic well with a magnetic stirrer. A three-electrode configuration, the same as that mentioned above, was used for experiments.

Microelectrophoresis. The LbL encapsulation process was monitored by measuring the microelectrophoretic mobility of the coated particles with a ZetaPlus ζ potential analyzer (Brookhaven). A 5 μL aliquot of suspended encapsulated microcrystals was examined by taking an average of 10 measurements at stationary level. The mobility (μ) was converted into electrophoretic potentials (ζ) by using the Smoluchowski relation $\zeta = \mu h/\epsilon$, where η and ϵ are the viscosity and the permittivity of the solution, respectively.

Particle Size Analysis. The particle size distribution of hand-milled ferrocene microcrystals was determined by a particle size analyzer (Coulter Delsa 440) based on light scattering measurement.

Scanning Electron Microscopy. A diluted microcrystal or hollow polymeric capsule sample was air-dried on a glass substrate and deposited with a gold film. Micrographs were taken with a Philips LX-30 scanning electron microscope (SEM) operated at 15 kV.

RESULTS AND DISCUSSION

Voltammetric and Amperometric Calibration of Ferrocene. The electrochemical properties of ferrocene were studied by cyclic voltammetry. Cyclic voltammograms of ferrocene solution with concentrations ranging from 4 to 300 μM were recorded. Ferrocene undergoes a reversible one-electron redox reaction and resulted in a peak cathodic current of +250 mV and a peak anodic currently of +360 mV. Amperometric detection of ferrocene was performed at +250 mV with a glassy carbon working electrode. It shows a response to ferrocene concentration was linear in the range of 0.5−22 μM with the regression equation of $y = 9.8291x + 7.3635$ ($R^2 = 0.992$), where y is the current signal (nA) and x is the ferrocene concentration (μM).

Preparation and Characterization of Encapsulated Microcrystals. The ferrocene microcrystals have irregular shape with a mean particle size distribution of 1 μm in diameter (Figure 2). The encapsulation of ferrocene microcrystals was achieved by

(22) Chan, C. P. Y.; Bruemmel, Y.; Seydack, M.; Sin, K. K.; Wong, L. W.; Merisko-Liversidge, E.; Trau, D.; Renneberg, R. *Anal. Chem.* **2004**, *76*, 3638−3645.

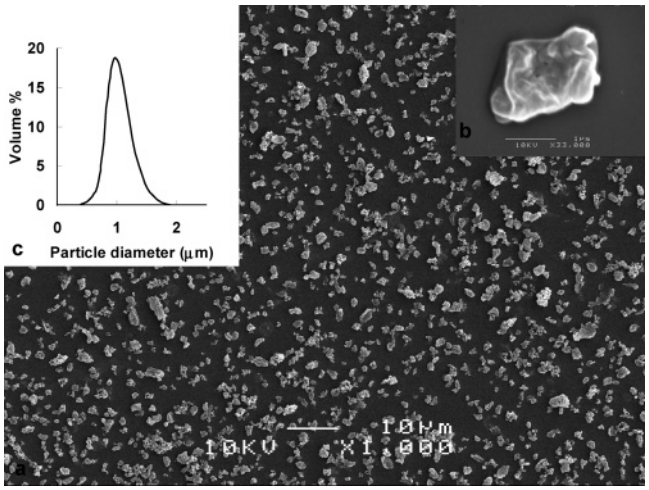

Figure 2. (a) SEM micrograph of hand-milled ferrocene microcrystals. (b) Surface morphology of a single ferrocene microcrystal. (c) Particle size distribution curve of the ferrocene microcrystals.

alternate deposition of polyelectrolyte multilayers via LbL technique. The consecutive assembly of polyelectrolyte multilayers onto the microcrystals surface was monitored by microelectrophoresis measurements. The electrophoretic mobility of the microcrystals after deposit with a positively charged polyelectrolyte (PAH), and subsequently polyelectrolyte of alternating charge (PSS), was measured. The sign of the ζ potential indicates the positive or negative surface charge of the ferrocene microcrystals, and the magnitude indicates the stability of the successive polyelectrolyte-coated microcrystal suspension. Ferrocene microcrystals exposed to PSS showed an average ζ potential of ≈ -37 mV, while exposed to PAH, an average ζ potential of $\approx +35$ mV. The alternate positive and negative ζ potential pattern confirmed the stepwise LbL assembly of polyelectrolyte multilayers onto ferrocene microcrystal templates.

Biofunctionalization and Characterization of LbL-Coated Microcrystals. The microcrystals were functionalized for immunodetection by assembling Gt α M-IgG molecules onto the LbL-encapsulated microcrystal surfaces. The conjugation of Gt α M-IgG was achieved by electrostatic adsorption process. Assembling of proteins by simple adsorption process has the advantage of minimizing protein denaturation during the conjugation process. The sensitivity of an immunoassay is mainly determined by the ratio between signal-generating molecules that conjugated to an antibody. Therefore, the Gt α M-IgG surface coverage on the encapsulated microcrystal and the signal-generating molecules to the Gt α M-IgG ratio were studied.

The IgG surface coverage of the encapsulated microcrystals prepared by incubating the encapsulated microcrystals with a solution of different initial Gt α M-IgG concentration was studied by spectrophotometric measurement at 280 nm. Encapsulated microcrystals with a concentration of 24.5 mg mL^{-1} were incubated with Gt α M-IgG solutions with various concentrations at room temperature for 30 min. The initial concentrations of Gt α M-IgG solution, the corresponding percentage of Gt α M-IgG molecule adsorbed, and the Gt α M-IgG surface coverage are summarized in Table 1. The theoretically calculated surface coverage value for a closely packed Gt α M-IgG monolayer is in the range of 2.0−5.5 mg m^{-2}, depending on the different

Table 1. Relationship between Initial Gt α M-IgG Concentrations; the Percentage of IgG Molecules Adsorbed and the Corresponding Gt α M-IgG Surface Coverage

initial Gt α M-IgG concentration (μg mL^{-1})	Gt α M-IgG adsorbed (%)	Gt α M-IgG surface coverage (mg m^{-2})	signal-generating molecules to antibody molecules ratio
150	42.1	1.60	1.25×10^5
300	38.5	2.93	6.83×10^4
600	29.3	5.05	3.95×10^4

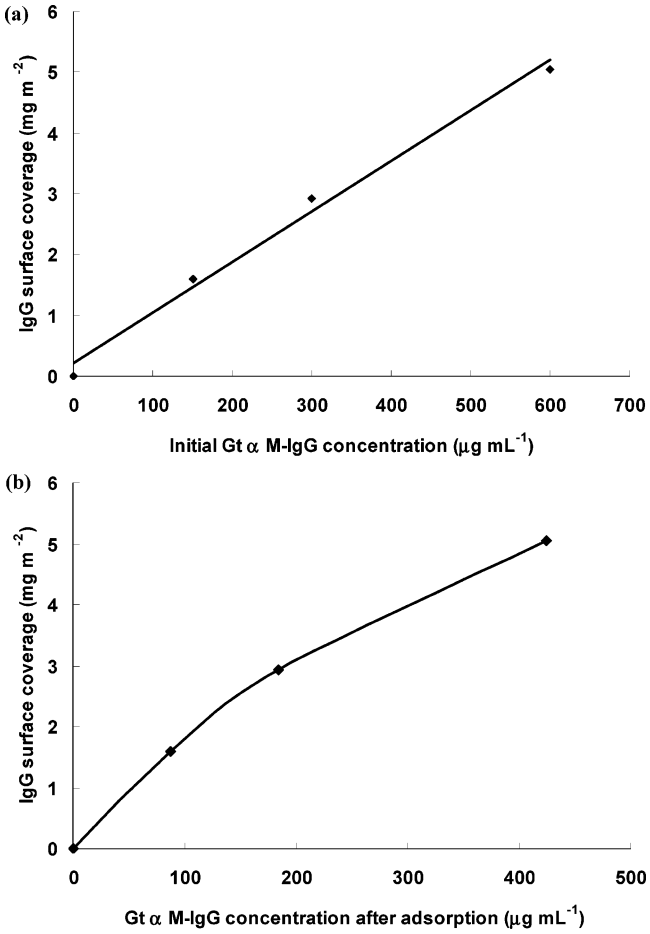

Figure 3. (a) Relationship between the initial Gt α M-IgG concentration and the Gt α M-IgG surface coverage. (b) Adsorption isotherms of Gt α M-IgG adsorbed on encapsulated microcrystal surfaces.

orientations of the IgG molecules.[23,24] This indicated a high Gt α M-IgG surface coverage was achieve under the adsorption conditions with an initial Gt α M-IgG concentration of 300 and 600 μg mL^{-1}, while a low Gt α M-IgG surface coverage resulted under the adsorption condition with an initial IgG concentration of 150 μg mL^{-1}. Moreover, the results showed a linear relationship between the initial Gt α M-IgG concentration and the Gt α M-IgG surface coverage with a slope of 0.0083 (Figure 3a), and the corresponding adsorption isotherms are shown in Figure 3b. This indicated the Gt α M-IgG surface coverage on the encapsulated

(23) Buijs, J.; Lichtenbelt, W. T.; Norde, W.; Lyklema, J. *Colloids Surf., B* **1995**, *5*, 11−23.
(24) Nakamura, M.; Ohshima, H.; Kondo, T. J. *Colloid Interface Sci.* **1992**, *149*, 241−246.

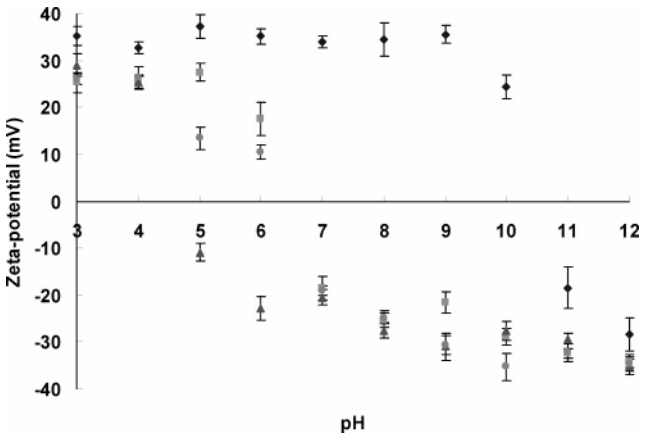

Figure 4. pH dependence of ζ potentials of encapsulated microcrystals with $(PSS/PAH)_4$ (rhombus), encapsulated microcrystals with Gt α M-IgG outer layer (square), encapsulated microcrystals with BSA outer layer (triangle), and encapsulated microcrystals with Gt α M-IgG outer layer followed by BSA adsorption (circle).

microcrystals increased with increasing initial concentration of the Gt α M-IgG solution, while the adsorption efficiency (percentage of Gt α M-IgG adsorbed) decreased. Furthermore, the IgG surface coverage does not reach a steady state upon initial Gt α M-IgG concentration of 600 μg mL^{-1}.

To calculate the number of signal-generating molecules to Gt α M-IgG (S/P) ratio, the number of signal-generating molecules in each microcrystal was calculated on the basis of the assumption that each microcrystal has a cubic morphology. From the data of the SEM micrographs and particle size analysis (Figure 2), the average dimension of the milled ferrocene microcrystals was about 1 μm × 1 μm × 1 μm. Therefore the number of ferrocene molecules within each encapsulated microcrystal was about 4.8×10^9, and the calculation was based on the following equation: number of ferrocene molecules $= (m/M)N_A = (a^3\rho/M)N_A$, where m is the mass of a single ferrocene crystal, M is the molecular weight of ferrocene (=186.04 g mol^{-1}), N_A is the Avogadro number ($=6.02 \times 10^{23}$), a is the dimension of a ferrocene crystal ($=1 \times 10^{-4}$ μm^3), and ρ is the density of the ferrocene crystal (=1.49 g cm^{-3}).[25] From the calculated number of signal-generating molecules per microcrystal and the number of IgG molecules adsorbed on each microcrystal, the S/P ratio was calculated to be in the range from 3.95×10^4 to 1.25×10^5. These values showed that the encapsulated microcrystal label system has 10^4-10^5 times higher S/P ratio when compared with the convention label system. The encapsulated microcrystal label system with a high S/P ratio provides a potential tool for developing a sensitive electrochemical immunoassay.

The conjugation of Gt α M-IgG molecules on the LbL-encapsulated microcrystals was characterized by electrophoresis measurements. LbL-coated microcrystals with and without protein conjugate were subjected to electrophoresis measurements under various pH conditions (Figure 4) (microcrystals with Gt α M-IgG surface coverage of 2.93 mg m^{-2} were used for the experiments). The results show that microcrystals coated with $(PSS/PAH)_4$ exhibited a positive surface charge at a pH range from 3 to 10, while the surface charge reversed to a negative value at a pH range from 11 to 12. For the encapsulated microcrystals conjugated with Gt α M-IgG molecules as the outermost layer; they exhibited a positive surface charge at a pH ranging from 3 to 6, while the surface charge reverse to a negative value at a pH ranging from 7 to 12. For microcrystals coated with $(PSS/PAH)_4$, the surface charge reversal occurred at a pH value between 10 and 11, which is close to the pK_a value of PAH (pK_a ∼ 10.6).[26] For the encapsulated microcrystals conjugated with Gt α M-IgG as the outermost layer, the surface charge reversal occurred at a pH value between 6 and 7, which is close to the isoelectric point of Gt α M-IgG molecules (IgG isoelectric point ∼ 6.8).[27] Similar results were reported by Nakamura et al. and Buijs et al., which showed that the isoelectric point of the protein-coated colloids is close to that of the native protein when the protein surface coverage is high.[23,24] From our results, microcrystals coated with an outer layer of Gt α M-IgG showed an isoelectric point value of about 6.0, which is slightly lower than the value of the native protein which is about 6.8. These results indicate the conjugation of Gt α M-IgG molecules onto the encapsulated microcrystal surfaces through adsorption process. Although a high Gt α M-IgG surface coverage was obtained, the results from the relationship between initial Gt α M-IgG concentration and the Gt α M-IgG surface coverage indicated saturation does not occur. This may be due to the reason that microcrystal surfaces with fully covered Gt α M-IgG are not achieved (Figure 3). The uncovered capsule surfaces will cause nonspecific binding during the immunoassay, and thus blocking of the uncovered capsule surfaces is necessary.

To block the uncovered microcrystal surfaces, BSA was adsorbed onto the microcrystal surfaces after the Gt α M-IgG conjugation process. BSA is the most commonly used blocking reagent in the immunoassay which can lower the nonspecific binding activities. The blocking of the microcrystals surface by BSA was performed through the adsorption process. Antibody-conjugated microcrystals with Gt α M-IgG surface coverage of 5.05 mg m^{-2} were incubated with a 1% (w/v) BSA solution followed by washing steps. The adsorption of BSA onto the microcrystal surface was characterized by electrophoresis studies. The encapsulated microcrystals with Gt α M-IgG conjugate followed by BSA adsorption were subjected to electrophoresis measurements under various pH conditions (Figure 4). The ζ potential results showed two changes in the ζ potential value occurred. The first change appears at a pH value between 3 and 5, while the second change appears at the pH value between 6 and 7. The first change in the ζ potential value indicates the adsorption of BSA onto the microcrystal surface with a value close to the isoelectric point of BSA (isoelectric point of BSA ∼ 4.9),[23] while the second change in the ζ potential value indicate the adsorption of Gt α M-IgG molecules. More evidence for the adsorption of BSA onto microcrystal surfaces was given by performing electrophoresis measurement of encapsulated microcrystals coated with BSA as the outermost layer. This result showed a surface charge reverse occurred at a pH value between 4 and 5, which indicates the adsorption of BSA on the microcrystal surfaces. For microcrystals

(25) TheFreeDictionary.com, http://encyclopedia.thefreedictionary.com/Ferrocene.

(26) Riegler, H.; Essler, F. *Langmuir* **2002**, *18*, 6694−6698.

(27) Ariga, K.; Lvov, Y. M. Self-assembly of functional protein multilayers: From planner films to microtemplate encapsulation. *Biopolymers at Interfaces*; Dekker: New York, 2003; pp 367−391.

with Gt α M-IgG conjugate followed by BSA blocking, the first change causes a slight drop in the magnitude of the ζ potential value, while there is no surface charge reverse occurring. This is because the surface coverage of BSA was low when compared with Gt α M-IgG. At a pH value below 4.9, both BSA and Gt α M-IgG molecules are protonated and therefore microcrystal surfaces were positively charged. At a pH value between 4.9 and 6.8, BSA molecules are deprotonated and become negatively charged while the IgG molecules are protonated. Because the Gt α M-IgG molecules surface coverage was higher than the BSA surface coverage, the overall charge of the microcrystal surfaces remains positive and the slight drop in the magnitude of the ζ potential value results from the deprotonation of the BSA molecules. At a pH value above 6.8, both BSA and Gt α M-IgG molecules were deprotonated and resulted in microcrystal surface charge reversal.

Utilization of Biofunctionalized Microcrystals for Immunoassay. A sandwich immunoassay for quantitative detection of M-IgG was performed in a microtiter plate with ferrocene microcrystal labeled detector antibodies. After performing the immunoassay, DMSO was added to dissolve the ferrocene microcrystals. The resulting electrochemical signal-generating molecules were immediately released through the permeable capsule wall into the outer environment and measured with amperometric measurement. Figure 5 shows the calibration curve of M-IgG detection with the ferrocene microcrystal labeling system with different Gt α M-IgG surface coverage. For the microcrystals with Gt α M-IgG surface coverage of 2.93 and 5.05 mg m^{-2}, a linear detection range for M-IgG from 0 to 25 μg L^{-1} with correlation coefficients $R^2 = 0.987$ and $R^2 = 0.985$, respectively, was observed. Saturation was observed at M-IgG concentrations above 50 μg L^{-1}. While for a microcrystal with a Gt α M-IgG surface coverage of 1.60 mg m^{-2}, a linear detection range for M-IgG was observed from 0 to 100 μg L^{-1} with a correlation coefficient $R^2 = 0.975$. Saturation was observed for M-IgG concentrations above 100 μg L^{-1}. The sensitivities of the microcrystal-labeled immunoassay with microcrystals having Gt α M-IgG surface coverages of 1.60, 2.93, and 5.05 mg m^{-2} were found to be 0.42, 3.76, and 3.93 nA μg^{-1} L^{-1}, respectively. It was surprising that, from the previous calculation on the S/P ratio, microcrystals with the Gt α M-IgG surface coverage of 1.60 mg m^{-2} showed the highest S/P ratio. However, the results showed that, for microcrystal label systems with high S/P ratio, the sensitivity of the immunoassay drop when compared with the microcrystal label system with lower S/P ratio. We may explain the effect by the affinity between the antigen (M-IgG) and the biolabels (microcrystals conjugated with Gt α M-IgG). In conventional redox-active molecules or an enzymes-based antibody label system, the force required to maintain the labeled antibodies and antigens interaction is small. When we consider the microcrystal-based antibody label system, a large force is required to maintain the biointeraction between the antibody-conjugated microcrystals and the antigens. Although each microcrystal label carries about $2 \times 10^5 - 4 \times 10^5$ antibody molecules (assuming the microcrystal has a full surface coverage), the antibody surface coverage is an important parameter to determine the total force that is available for the interaction between the antibody-conjugated microcrystals and the antigens. As a result, microcrystals with Gt α M-IgG surface coverages of 2.93 and 5.05 mg m^{-2} which contain a high coverage of IgG monolayer (as the theoretically calculated surface coverage value for a closely packed Gt α M-IgG monolayer is in the range of 2.0−5.5 mg m^{-2}, depending on the different orientation of the IgG molecules[23,24]) give a higher sensitivity immunoassay when compared with microcrystals having a lower Gt α M-IgG surface coverage. By considering the immunoassay performed with microcrystals having Gt α M-IgG surface coverage of 5.05 mg m^{-2}, the detection limit that is the minimum distinguishable analytical signal was calculated to be 2.82 μg L^{-1} (2×10^{-11} mol L^{-1}) based on three times the standard deviation of the blank signals divided by the calibration sensitivity (slope of the linear correlation curve).

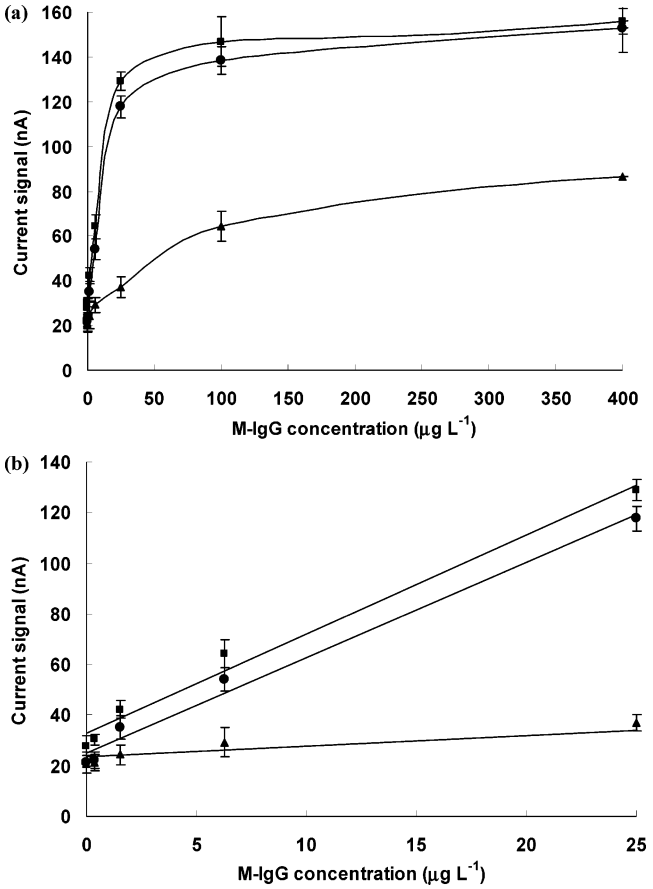

Figure 5. (a) Sandwich electrochemical immunoassay for M-IgG detection with microcrystal biolabels having a Gt α M-IgG surface coverage of 1.60 (triangle), 2.93 (circle), and 5.05 mg m^{-2} (square). (b) Calibration curves of the same electrochemical immunoassay with M-IgG concentration ranging from 0 to 25 μg L^{-1}.

CONCLUSION

A new approach for electrochemical immunoassays by using encapsulated ferrocene microcrystals as the label system has been demonstrated. Ferrocene microcrystals were encapsulated within an ultrathin capsule. The polymeric capsule wall provides a stable interface for antibody conjugation. The protein surface coverage of ferrocene microcrystals incubated with antibody solutions with different initial concentrations were found to be 1.60, 2.93, and 5.05 mg m^{-2}, respectively. The corresponding S/P ratios were found to be 1.25×10^5, 6.83×10^4, and 3.95×10^4, respectively. Our results showed that although the S/P ratio is an important

parameter in determining the sensitivity of a bioassay, the antibody surface coverage on the microcrystals plays an important role in microcrystal-based immunoassays. The ferrocene microcrystal biolabel system provides a simple method to conduct electrochemical immunoassay with high detection sensitivity. The microcrystal-based immunoassays performed with microcrystal biolabels having a Gt α M-IgG surface coverage of 5.05 mg m^{-2} showed a good sensitivity of 3.93 nA μg^{-1} L^{-1} for the detection of M-IgG with a linear range from 0 to 25 μg L^{-1}. The detection limit was calculated to be 2.82 μg L^{-1} (2×10^{-11} mol L^{-1}). Our approach provides an alternative biolabel system to perform electrochemical immunoassay.

Received for review October 9, 2004. Accepted February 7, 2005.

AC048505L